Mass transfer and photocatalytic degradation of leather dye using TiO₂/UV

REGINA DE FÁTIMA PERALTA MUNIZ MOREIRA[1], TICIANE POKRYWIECKI SAUER[1],
LEONARDO CASARIL[1] and EDUARDO HUMERES[2]
[1]*Department of Chemical and Food Engineering, Federal University of Santa Catarina Campus Universitário,
Trindade, 88040-900, Florianópolis – Santa Catarina, Brazil*
[2]*Department of Chemistry, Federal University of Santa Catarina Campus Universitário, Trindade, 88040-900,
Florianópolis – Santa Catarina, Brazil*
(*author for correspondence, e-mail: regina@enq.ufsc.br)

Abstract

The global process of heterogeneous photocatalytic oxidation can be described in consecutive steps of mass transfer, adsorption, reaction and desorption. Although such a deseription normally only considers the reactions in the aqueous solution, some compounds are degraded by photogenerated holes in the surface of the solid. In this work, the photocatalytic degradation of a leather dye, Direct Black 38, was studied as a model compound to elucidate the steps during the photocatalytic degradation. The mass transfer coefficients were evaluated through the description of the adsorption kinetics using the film and pore diffusion model. The equilibrium of adsorption was described according to the Langmuir model. Under irradiation, the degradation of the dye was measured and a pseudo-first order kinetic law was used to depict the reaction. The Weiz-Prater criterion was used to determine the rate controlling step of the reaction with the result that no diffusion limitations for the reaction existed. The characterization of the solid after adsorption and after desorption showed the presence of the reaction's intermediate species.
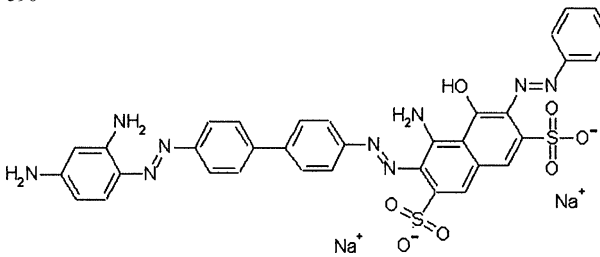
Nomenclature

b	Langmuir equilibrium contant
C_B	concentration of dye in the aqueous phase at time t
C_e	concentration of dye in the aqueous phase at equilibrium
C_i	concentration of dye in the aqueous phase inside the particle
C_s	concentration of dye at surface of the solid
C_{WP}	Weisz–Prater parameter
D_{ef}	effective diffusion coefficient
D_M	molecular diffusivity
K_f	mass transfer coefficient in the hydrodynamic film around the particle
M	molecular weight
q_e	concentration of dye in the solid phase at equilibrium
q_m	monolayer coverage capacity
q_0	maximum amount of dye adsorbed in the solid phase
r	radial position in relation to the center of the particle
R	particle radius
$-r$	photocatalytic degradation rate
t	time
T	temperature
V_m	molar volume
τ	tortuosity
μ	viscosivity
ϕ	constant ($H_2O = 2.27$)
ε_p	particle porosity
ρ_p	specific gravity of the solid

1. Introduction

Every day in the world, about 400 tonnes of dyes find their way into the environment, primarily dissolved or suspended in water and causing a major environmental impact. Effluent treatment processes for dye-containing effluents from the textile, pulp and paper industries, tanneries, etc., are currently capable of removing about only half the dyes lost in residual liquors [11], since the majoriy of these compounds are not readily biodegraded by the conventional effluent treatment methods [22]. Colored organic substances generally impart only a

Table 1. Information regarding the direct dye

Name	Direct Black 38
CAS number	CAS 1937-37-7
Molecular weight, g mol^{-1}	781
Molar volume, cm^3 mol^{-1}	918.8
Specific gravity, g cm^{-3}	0.85
λ_{max} (nm)	590
Chemical structure	

small fraction of the total organic load in any given waste water; however, their high degree of color is easily detectable and detracts from the aesthetic value of rivers, streams, etc., appart from inhibiting natural photosynthetic processes [11].

New or more efficient wastewater treatment technolgies are being studied to degrade complex refractory molecules into simpler molecules. Heterogeneous photocatalytic degradation is gaining importance in the area of wastewaster treatment, since this process results in complete mineralization operating under mild conditions of temperature and pressure.

Among the various photocatalysts available, the most active is TiO$_2$ Degussa P-25 (hybrid mixture of rutile and anatase forms), which generally gives better degradation efficiencies of the photocatalytic process [33, 44]. The surface area and number of active sites of the catalyst are important parameters, since the adsorption of pollutants plays an important role in the global process.

The overall process can be seen as consisting of five independent steps [55]: transfer of the reactants in the fluid phase to the surface; adsorption of a least one of the reactants; reaction in the adsorbed phase; desorption of the product(s); removal of the products from the region of the interface.

Some authors have reported that the photocatalytic reaction occurs in the adsorbed phase, and the Langmuir–Hinshelwood mechanism (L–H) has largely applied. There is no consensus about the controlling rate step, although some authors [22, 66] have reported that the adsorption step controls the rate. More complex models has also been proposed including the radiation transfer equation, but they can be simplified in certain cases to the L–H model [77].

Several factors can affect the photocatalytic degradation rate and the mass transfer of the pollutant from the liquid phase to the external surface of the particle, and the diffusion inside the particle is unsufficiently discussed in the literature. In this work, we evaluate the kinetics of the photocatalytic degradation of a direct dye

using TiO$_2$ under UV irradiation in a slurry reactor. Attention is focused on the effect of the adsorption on the photocatalytic reaction and the mass transfer coefficients are evaluated to determine the rate controlling step.

2. Experimental section

Direct Black 38, a dye extensively used in the leather industry, was used as model compound. Table 1 shows the CAS number, molecular mass, structure, and the wavelength at which maximum absorption of light occurs, λ_{max}.

Degussa P-25 titanium dioxide was used as the photocatalyst. It is mostly in the anatase (80% anatase form and 20% rutile) and has a B.E.T. surface area of 50 m^2 g^{-1} corresponding to a mean particle size of ca. 30 nm and mean pore diameter of about 6.9 nm.

2.1. *Sorption equilibrium and kinetics studies*

A series of fixed volumes (200 ml) solutions with predetermined initial dye concentrations were prepared and brought into contact with predetermined masses (1 g) of TiO$_2$. The flasks were sealed and agitated in the shaker (60 rev min^{-1} shaking rate) at a constant temperature of 25 $\pm$ 1 °C for 24 h until equilibrium was reached. All samples were analyzed using a Shimadzu 1650C UV spectrophotometer. The amount of adsorbed dye on the TiO$_2$ surfacewas determined by mass balance.

Batch kinetics experiments were used to evaluate the mass transfer coefficients for the adsorption of dye on the TiO$_2$ surface. The adsorber vessel was a 2l reactor that was continuously stirred (60 rev min^{-1}), containing the catalyst in suspension in the aqueous solution, in dark conditions.

An aliquot of the aqueous solution was taken at various time intervals, centrifuged and filtered through

a PVDF membrane (0.22 μm) before analysis. The concentration of dye in aqueous solution was determined by UV–Vis spectrometry at 590 nm.

2.2. Photocatalytic degradation studies

The design of the batch reactor has been described in previous papers [88]. The reactor was an annular reactor irradiated by a 80 W high-pressure mercury vapor lamp and the light intensity was 1.64×10^{-4} Einstein min^{-1} [99]. The UV lamp was surround by a quartz thimble in the center of the reactor to ensure homogeneous radiation field inside the reactor. To avoid the heating of the solution, water was circulated through a cylindrical jacket around the plunging tube. The volume of the aqueous solution of dye was 2 l to which 2 g of TiO$_2$ powder was added. The degradation was carried out at 293 K by stirring the solution in the dark for 24 h to reach equilibrated adsorption.

The continuous system for photocatalytic degradation of the dye was an annular reactor (Trojan UV Max^{TM} – E) illuminated by a 15 W UV lamp, whose irradiation spectrum was in the range 300–410 nm and whose maximum emission was at 355 nm. The experiments were carried out passing the aqueous solution at different flowrates, in order to give different times. Aliquots were taken at the of the reactor, centrifuged and filtered by PVDF 22 μm membrane prior to the analyses to remove TiO$_2$ powder.

2.3. Analyses

The disappearance of the dye was analyzed by UV–Vis spectrophotometry (Shimadzu 1650C), recording the spectra over 190–1100 nm. Calibration plots based on Beer–Lambert's law were established, relating the absorbance to the concentration. The decolorization was determined at 590 nm, the maximum of absorbance.

After reaction, the filtered solids (dye-TiO$_2$ complexes) were analyzed by FTIR spectrometry, after drying in air at 70 °C. FTIR spectra were obtained ex situ employing a Perkin-Elmer FTIR spectrometer and a KBr beam splitter. Spectra were obtained with a 32-scan data acquisition at a resolution of 4 cm^{-1}. In all cases, spectra were obtained from the sample exposed to the atmosphere at room temperature. Titanium dioxide powder, subjected to a similar pretreatment (suspended in water, filtered, dried, etc.), was used as a background reference.

2.4. Toxicity

Artemia salina cysts were incubated in artificial seawater illuminated by a tungsten filament light and gently sparged with air at 25 °C. After 24 h, hatched A. Salina cysts were transferred to fresh artificial seawater and incubated for a farther 24 h under artificial light with air sparging. Subsequently, an aliquot of 0.5 ml of treated wastewater and 5 ml of fresh seawater was poured into wells in polyestyrene microtiter plates, and then 7 to 10 A. Salina nauplii were placed in each well. Deaths were recorded periodically after incubating at 25 °C for 24 h [1010, 1111].

3. Results and discussion

3.1. Direct Black 38 adsorption TiO$_2$

Figure 1 illustrates the adsorption isotherm of Direct Black 38 over TiO$_2$, where q_e is plotted as a function of C_e, in the dark. C_e is the concentration of Direct Black 38 remaining in the bulk solution upon the attainment of adsorption/desorption equilibrium in the dark, and q_e is the concentration of Direct Black 38 adsorbed in the solid (For symbols see nomenclature and definitions).
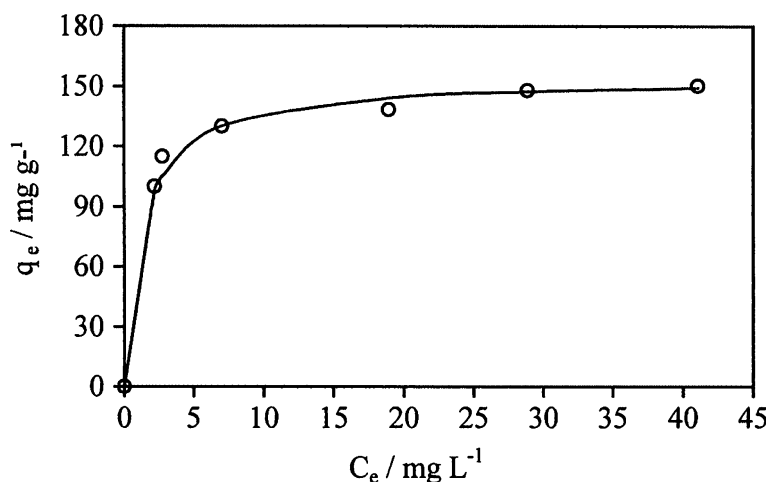

Fig. 1. Direct Black 38 adsorption isotherm on TiO$_2$ (pH 2.5; T = 25 °C). Circle data points correspond to the experimental data and the line is the fitting to the Langmuir model.

The isotherm showed a type of L-shape according to the classification of Giles et al. [1212] The L-shape isotherms mean that there is no strong competition between the solvent and the dye to occupy the TiO$_2$ surface sites. The data obtained from the adsorption experiments were fitted to the Langmuir equation [1313]:

$$q_e = \frac{q_m b C_e}{1 + b C_e} \quad (1)$$

where C_e is the concentration of the dye in solution at equilibrium, q_e is the amount of dye adsorbed per unit weight of the catalyst at equilibrium, and b is the Langmuir adsorption constant, and Q_0 is the amount of dye adsorbed corresponding to monolayer coverage. The fitting of experimental data to the Langmuir model resulted in $q_{e=154}$ mg g^{-1} and $b = 0.78$ l mg^{-1}.

The amount of dye adsorbed on the TiO$_2$ surface at different pH values (not shown) decreased as the pH increased and was negligible at neutral or alkaline conditions.

3.2. Kinetics of adsorption of Direct Black 38 on TiO$_2$

Several models of adsorption kinetics [1414–1717], based on diffusional mass transport, have been reported in the literature. Spahn & Schlünder [1414] developed the film-pore diffusion model based on the unreacted shrinking core mass transfer model of Yagi and Kunii [1919]. This model assumes that an external and internal transfer resistance controls the adsorption rate. Therefore, the adsorption starts at the particle surface forming a saturated zone, which moves inwards at a defined rate. During the entire adsorption time, there is an unreacted core, shrinking in size as the adsorption proceeds [11].

The model selected in this paper for predicting concentration versus time-decay curves is based on external film mass transport and pore diffusion. In the heterogeneous adsorption sequence, mass transfer of dye molecules first takes place from the bulk fluid to the external surface of the spherical particles. The dye molecules then diffuse from the external surface into and through the pores with the particle, within the adsorption taking place only on the solid surface of the pores.

The mass balance in the adsorbent spherical particle is given by Equation 2.

$$\varepsilon_p \cdot \frac{\partial C_i}{\partial t} = D_{ef} \cdot \left(\frac{\partial^2 C_i}{\partial r^2} + \frac{2}{r} \frac{\partial C_i}{\partial r} \right) - \frac{\partial q_i}{\partial t} \quad (2)$$

The initial and boundary conditions are given by Equations 3–5.

$$t = 0 \quad C_i = 0 \quad (3)$$

$$r = 0 \quad \frac{\partial C_i}{\partial r} = 0 \quad (4)$$

$$r = R \quad \frac{dC_i}{dr} = \frac{K_f}{D_{ef}} \cdot (C_i - C_B) \quad (5)$$

Since the equilibrium isotherm can be described according to the Langmuir model:

$$\frac{\partial q_i}{\partial t} = \frac{q_0 K_d}{(K_d + C_i)^2} \cdot \frac{\partial C_i}{\partial t} \quad (6)$$

By combining Equations 2 and 6:

$$\frac{\partial C_i}{\partial t} \cdot \left(\varepsilon_p + \frac{q_0 \cdot K_d}{(K_d + C)^2} \right) = D_{ef} \cdot \left(\frac{\partial^2 C_i}{\partial r^2} + \frac{2}{R} \cdot \frac{\partial C_i}{\partial r} \right) \quad (7)$$

The dimensionless parameter, Biot number (Bi), defines a relative ratio between the mass transfer in the film around the particle and the mass transfer inside the particle (Equation 8)

$$Bi = \frac{K_f R}{D_{ef}} \quad (8)$$

where R is the particle radius. When the Biot number is higher than 100, the major resistance to mass transfer is within the adsorbent particle rather than external to the particle.

The effective diffusivity in the pore diffusion model should be constant and equal to the pore diffusivity, which is also a function of molecular diffusivity, porosity and tortuosity, defined in Equation 9. [11] The effective diffusivity accounts for the fact that the diffusion paths are tortuous, the pores are of varying cross-sectional areas, and not all of the area normal to the direction of the flux is available (i.e., void) for the molecules to diffuse [11].

$$D_{ef} = \frac{D_M \varepsilon_p}{\tau} \quad (9)$$

The tortuosity is defined as the relationship between the actual distance a molecule travels between two points inside the pores and the shortest distance between those two points [1919].

Porosity of the catalyst P25 TiO$_2$ (ε_p) was taken as 0.34 [2020] and the tortuosity (τ) is assumed to be equal to 12 [2121]. The molecular diffusivity, D_M, of the direct

Table 2. Predicted results for the adsorption of Direct Black 38 onto TiO$_2$ using theoretical film and pore diffusion model (pH 2.5)

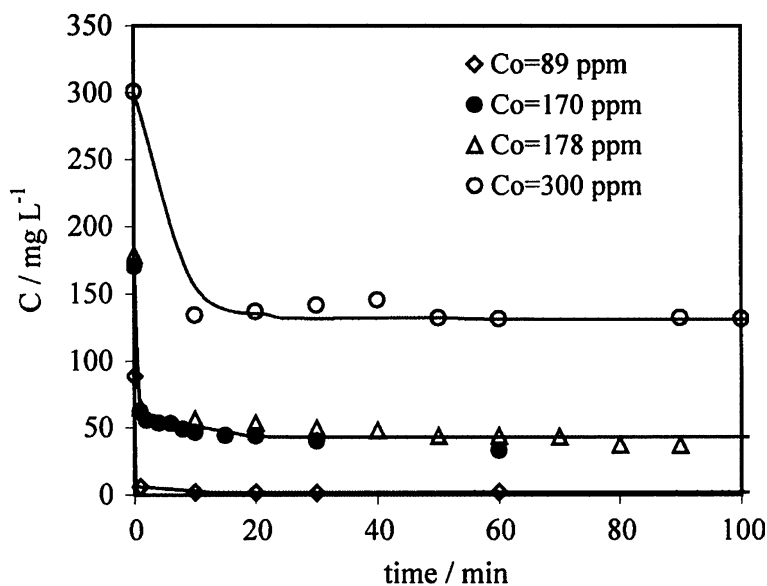| C_0/ppm	D_{ef}/cm^2 s^{-1}
90	1.23×10^{-8}
178	1.08×10^{-8}
300	1.38×10^{-8}
–	5.5×10^{-8a}

[a]Calculated according to Equation 9.

Fig. 2. Kinetics of sorption of Direct Black 38 on TiO₂ at pH 2.5 with different initial dye concentrations (circles – experimental data; lines – theoretical model) ([TiO₂ = 1 g l^{-1}).

dye was estimated using the Wilke–Chang expression (Equation 10), and it is shown in Table 2.

$$D_M = \frac{(7.4 \cdot 10^{-8})(\phi M)^{0.5} T}{\mu V_m^{0.6}} \qquad (10)$$

The film diffusion coefficient, K_f, was evaluated according to Equation 11 ($K_f = 4.1 \times 10^{-2}$ cm s^{-1}).

$$V\left[\frac{dC}{dt}\right]_{t=0} = -K_F a(C - C_s)_{t=0} \qquad (11)$$

Figure 2 shows the decay curves of the sorption of dye at pH 2.5 with different initial dye concentrations. The curves are generated by solving Equations 2–7, using the best-fit values of D_{ef} that minimize the error (ARE) between the experimental time, t_{exp}, and the calculated time from the adsorption model, t_{cal}. The D_{ef} values for each initial dye concentration are given in Table 2.

$$ARE = \frac{100}{n} \sum_{i=1}^{p} \left| \frac{t_{cal} - t_{exp}}{t_{exp}} \right|_i \qquad (12)$$

Figure 2 shows an excellent agreement between predicted and experimental data, and the adjusted D_{ef} values are similar to that evaluated by Eq. 10, within the experimental error, and independent on the initial dye concentration (Table 2).

The Biot number is high (>100) and indicates that the film around the particle has negligible resistance to mass transfer of dye to the particle surface [1818].

3.3. *Kinetics of decolorization of Direct Black 38*

The disappearance of the dye molecules was negligible by direct photolysis. A decolorization of dye could only be observed with the simultaneous presence of titania and UV-light.

Figure 3 presents the degradation of dye, in solutions containing different concentrations of the starting compound and 1.0 g l^{-1} of TiO₂ at pH 2.5, as a function of the illumination time. The decolorization of Direct Black 38 proceeds in a shorter time period at lower concentrations of the dye, as expected. The quasi-exponencial decay observed during the degradation indicates a pseudo-first order kinetics.

A quicker degradation was obtained in the discontinuous reactor than in the continuous reactor, because the radiation source was more powerful in the discontinuous reactor (employing UV lamps of 80 and 15 W in discontinuous and continuous reactors, respectively). The plot $-\ln (C/C_0)$ versus time was linear and the pseudo-first order constant was 3.6×10^{-3} and 4.4×10^{-3} min^{-1}, in the annular continuous reactor and in the discontinuous reactor, respectively.

The Weisz–Prater criterion (Equation 13) for internal diffusion was applied in order to evaluate the effect of the internal diffusion on the decolorization rate. [1919]

$$C_{WP} = \frac{(-r)\rho_p R^2}{D_{ef} C_s} \qquad (13)$$

If $C_{WP} << 1$ there are no diffusion limitations and consequently no concentration gradient exists within the particle. When $C_{WP} >> 1$, internal diffusion severely limits the reaction. Since the mass transfer in the film around the particle was a fast step, we assumed that C_s, the concentration of dye in the external surface of the particle, was equal to the concentration of dye in the bulk. The Weisz–Prater parameter, C_{WP}, was much less than 1, indicating that there was no kind of diffusional limitation during the reaction.
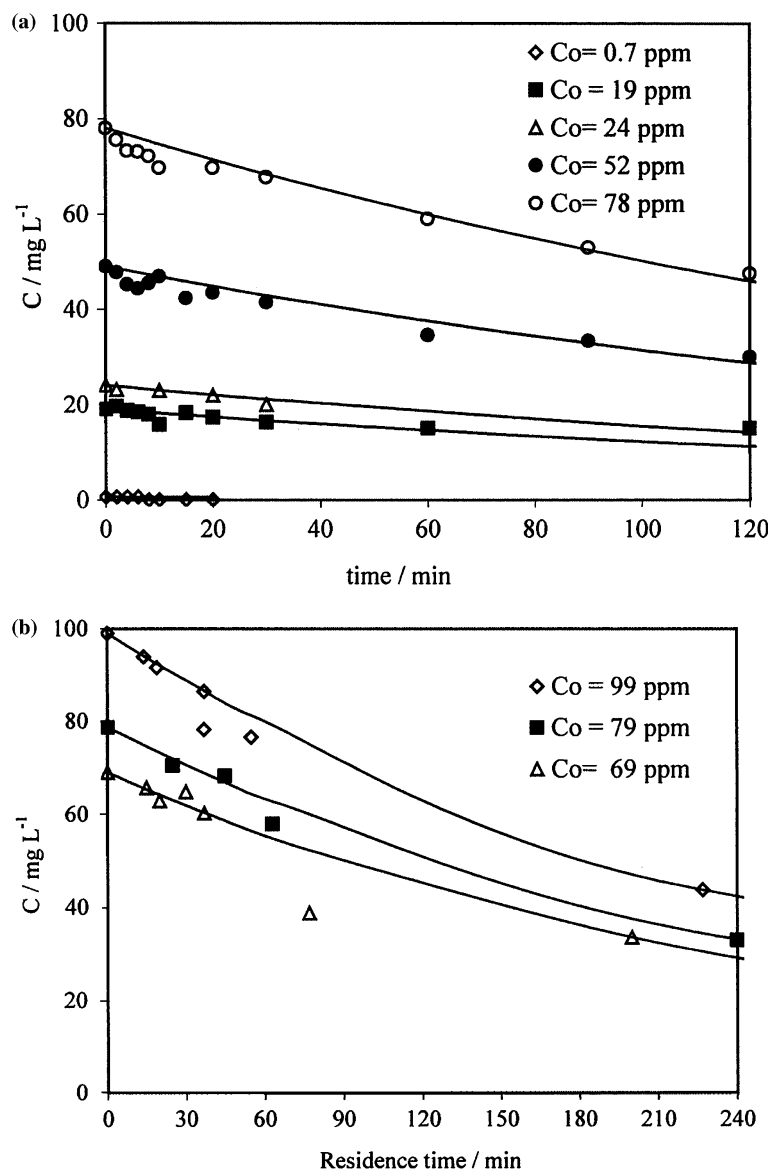
Fig. 3. Kinetics of decolorization for differential initial concentration of dye (a) Discontinuous reactor equipped with a UV lamp power 80 W; (b) annular continuous reactor equipped with a UV lamp power 15 W (Lines represent the pseudo-first order kinetic model; pH 2.5, $T = 25\ °C$; $[TiO_2] = 1\ g\ l^{-1}$).

3.4. Spectral UV–Vis changes in the aqueous solution during the photocatalytic degradation

UV–Vis spectra obtained from the dye solution at pH 2.5 as a function of irradiation time are shown in Figure 4. The UV–Vis absorption of Direct Black 38 is characterized by one band in the visible region, with its maximum located at 590 nm and by one band in the ultraviolet region with its maximum located at 310 nm. These different peaks are attributed to the benzene and naphthalene rings substituted with SO_3^- and OH groups [2222].

The subsequent illumination of the aqueous suspension causes a continuous decrease of the intensities of the UV and Vis bands of Direct Black 38 with increasing irradiation time (Figure 4), which is not accompanied

with change in absorption maxima or by the appearance of new absorption bands in the UV–Vis region.

Change in absorbance at 254 nm (UV254) throughout the photocatalytic oxidation, representing the total aromatic content [2323] of the samples, is illustrated in Figure 5 for the initial 190 mg l^{-1} concentration of the dye using the continuous UV reactor (employing a UV power lamp 15 W). The aromatic content increases at the beginning of the reaction, suggesting the formation of intermediates from incomplete oxidation during the initial steps of the photocatalytic degradation. This behavior was also observed in the photocatalytic degradation of other organic compounds [2323, 2424] and suggests that partially degraded aromatic compounds are formed during the reaction. These intermediates are also degraded, but a
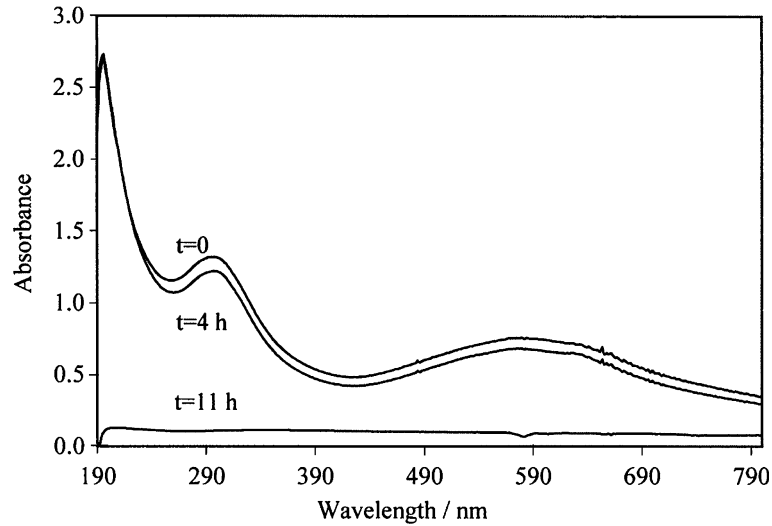
Fig. 4. UV–Vis spectra of Direct Black 38 as a function of irradiation time (pH: 2.5; [TiO$_2$]: 1 g l^{-1}; C_0: 200 ppm).

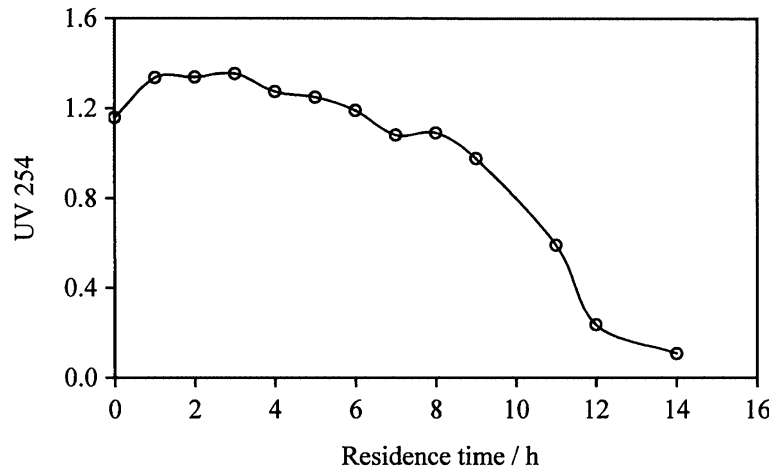*Fig. 5.* UV254 nm index as a function of time obtained in the continuous reactor (UV power lamp 15 W) (pH = 2.5, C_0 = 190 ppm, T = 25 °C, [TiO$_2$] = 1 g l^{-1}).
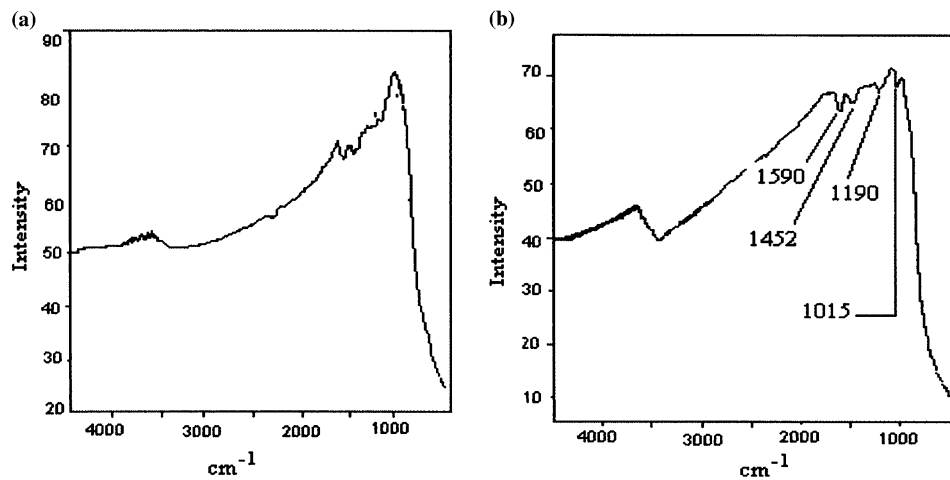

Fig. 6. FTIR spectra of TiO$_2$ under different treatments: (a) after adsorption of dye and reaction time t = 0; (b) collected after 3.7 h of reaction.

high residence time is required for their complete elimination.

3.5. FTIR spectra

The reaction of dye on the TiO_2 surface was accomplished using *ex situ* FTIR spectroscopy, and the spectra of TiO_2 collected at different reaction times are shown in Figure 6.

Figure 6a represents the spectrum of Direct Black 38 adsorbed onto the TiO_2 surface, before the UV irradiation, corresponding to the initial condition of the dye on the solid surface (reaction time = 0). The broad IR absorption in the 3600–2800 cm^{-1} range, with its maximum at 3450 cm^{-1}, arises from the superposition of the ν_{OH} mode of interacting hydroxyl groups (i.e., involved in hydrogen bonds) and the symmetric and antisymmetric ν_{OH} modes of molecular water coordinated to Ti^{4+} cations [2525]. The bands at 1590 and 1452 cm^{-1} are characteristic of phenyl rings, while the bonds Ti–O–Ti are responsible for bands in the region 900–950 cm^{-1} [2525].

The spectral changes observed in the FTIR of the catalyst collected after reaction for 3.7 h shows the progressive degradation of the organic molecules on the solid. It can be observed that the intensity of the bands in the ranges 1590 and 1452 cm^{-1} decreases, while new bands at 1190 and 1015 cm^{-1} have appeared. The presence of these new bands suggests that intermediate species are formed on the solid's surface from the oxidation/fragmentation of the dye molecules.

3.6. Toxicity

The accute toxicity of Direct Black 38 in aqueous solution using the bioassays with *Artemia salina* was evaluated in the concentration range 90–4000 mg l^{-1}. No mortality was measured in this concentration range.

The samples collected at different reaction times did not result in acute toxicity because no mortality was measured, indicating that the intermediate species are not toxic for *Artemia salina* or that they remain adsorbed on the solid surface.

3.7. Cost considerations

The costs of the treatment were evaluated according to EPA recommendation [2626] (Equation 14). This approach requires that information on key process variables, such UV dose and concentrations of oxidants and catalysts, should be generated by performing treatability studies. The approach was justified in this work because the photocatalytic degradation followed pseudo-first order kinetics.

$$\text{Total cost} = 1.45 \times \text{electric energy} + \text{chemical reagent costs} \tag{14}$$

The electric energy cost is calculated according to Equation 15.

$$\text{Electric energy cost}(US\$/m^3) = EE\left(\log\frac{C_{in}}{C_f}\right)\left(\frac{US\$}{kWh}\right) \tag{15}$$

where EE/O is the electrical energy required per unit volume of aqueous solution treated, C_{in} is the initial concentration, and C_f is the final concentration. In Brazil, the unitary cost of electric power (US\$ kWh^{-1}) is 0.1236 US\$ kWh^{-1}.

Using the kinetic data obtained in this work, the cost of achieving 50% of dye decolorization is US\$ 0.58 m^{-3}, considering the costs for electric energy, lamp replacements and reactor maintenance.

4. Conclusions

In this work, we studied the adsorption and photocatalytic degradation of a direct dye using TiO_2 as the catalyst. The equilibrium of adsorption was described according to the Langmuir model, and the monolayer coverage capacity was 154 mg of dye per gram of TiO_2. The kinetics of adsorption was elucidated using the film and pore diffusion model, and the results showed that the diffusion of the dye in the film around the particle was raster than the internal diffusion. The photocatalytic decolorization was described according to a pseudo-first order model and the rate constant depended on the UV light intensity. The rate constants were 3.6×10^{-3} min^{-1} and 4.4×10^{-3} min^{-1} using UV irradiation sources of 15 and 80 W, respectively.

The Weisz–Prater parameter was much less than 1, suggesting that there were no diffusional limitations for the degradation of the dye, and the controlling step was identified as being the reaction on the particle surface. During the irradiation, the intensity of the bands in the visible range decreased until their final disappearance due to the destruction of the cromophore group of the dye chemical structure.

The FTIR spectra of species adsorbed onto the solid during the reaction showed the progressive degradation of adsorbed dye molecules, and new bands appeared due to intermediate species being formed in the adsorbed phase.

Using the kinetic data obtained in this work, the cost of achieving 50% of dye decolorization is US\$ 0.58 m^{-3}, considering the costs for electric energy, lamp replacements and reactor maintenance.

References

1. K.H.J. Choy, J.F. Porter and G. McKay, *Chem. Eng. Sci.* **59** (2004) 501.
2. P.R. Gogate and A.B. Pandit, *Adv. Environ. Res.* **8** (2004) 501.
3. S. Sakthivel, B. Neppolian, B. Arabindoo, M. Palanichamy and V. Murugesan, *J. Sci. Ind. Res.* **59** (2000) 556.
4. S. Yamazaki, S. Matsunaga and K. Hori, *Water Res.* **35** (2001) 1022.
5. J.M. Herrmann, *Catal. Today* **53** (1999) 115.
6. N. Xu, Z. Shi, Y. Fan, J. Dong, J. Shi and M.Z.-H. Hu, *Ind. Eng. Chem. Res.* **38** (1999) 373.
7. G. Sagawe, R.J. Brandi, D. Bahnemann and A.E. Cassano, *Chem. Eng. Sci.* **58** (2003) 2601.
8. T.P. Sauer, G. Cesconetto Netto, H.J. José and R.F.P.M. Moreira, *J. Photochem. Photobiol. A Chem.* **149** (2002) 147.
9. R.F.P.M. Moreira, G. Cesconetto Netto, T.P. Sauer, H.J. José and E. Humeres, *J. Air Waste Manage. Asso.* **54** (2004) 77.
10. J.S. Metcalf and J. Linday, *Toxicon* **40** (2002) 1115.
11. R.S. Matthews, *Free Rad. Biol. Med.* **18** (1995) 919.
12. C.H. Giles, A.P. D' Silva and I.A. Easton, *J. Colloid Interface Sci.* **47** (1974) 766.
13. I. Langmuir, *J. Am. Chem. Soc.* **40** (1918) 1361.
14. H. Spahn and E.U. Schlünder, *Chem. Eng. Sci.* **30** (1975) 529.
15. I. Neretnieks, *Chem. Eng. Technol.* **46** (1974) 781.
16. G. McKay, M. El Geundi and M.M. Nassar, *Trans. Inst. Chem. Engrs Part B: Proc. Safety Environ. Protect.* **74** (1997) 277.
17. B. Chen, C.W. Hui and G. McKay, *Langmuir* **17** (2000) 740.
18. D.C.K. Ko, J.F. Porter and G. McKay, *Water Res.* **16** (2001) 3876.
19. O. Levenspiel, *Chemical Reaction Engineering* (Wiley, New York, 1962).
20. K. Vinodgopal, S. Hotchandani and P.V. Kamat, *J. Phys. Chem.* **97** (1993) 9040.
21. D. Chen, F. Li and A.K. Ray, *Catal. Today* **66** (2001) 475.
22. M. Karkmaz, E. Puzenat, C. Guillard and J.M. Herrmann, *Appl. Catal. B: Environ.* **51** (2004) 183.
23. I. Arslan and I.A. Balcioglu, *Dyes Pigments* **43** (1999) 95.
24. C.H. Kuo and C.H. Huang, *J. Hazard. Mater.* **41** (1995) 31.
25. A.J. Maira, J.M. Coronado, V. Augugliaro, K.L. Yeung and J. Soria, *J. Catal.* **202** (2001) 413.
26. EPA, Advanced Photochemical Oxidation Process, EPA/625/R-98/004 Washington, 1998.